International Journal of Rotating Machinery
1994, Vol. 1, No. 1, pp. 37–51
Reprints available directly from the publisher
Photocopying permitted by license only

Flow-Excited Turbine Rotor Instability

ANDREW D. DIMAROGONAS
W. Palm Professor of Mechanical Design, Washington University, St. Louis, MO 63130-4899

JULIO C. GOMEZ-MANCILLA
Electric Power Research Institute, Cuernavaca, Morelos, Mexico

The problem of steam whirl is one of the technological limits that now prohibit the development of power-generating turbomachinery substantially above 1 GW. Due to steam flow, self-excited vibrations develop at high loads in the form of stable limit cycles that, at even higher loads, deteriorate to chaotic vibration of high amplitude.

A mathematical model is developed for stability analysis and for the development of a rational stability criterion to be used at the design stage. The bearing nonlinearity is introduced in the form of high-order coefficients of a Taylor expansion of the perturbation forces for fixed-arc slider bearings and employing nonlinear pad functions for the tilting pad bearings. The flow excitation is introduced in the form of follower force gradients related to the flow and the power generated.

The study of the stable and unstable limit cycles, and the stability of the system in the large, beyond the linear analysis currently utilized, is done analytically for the De Laval rotor and numerically with finite element analysis of typical turbomachinery rotors.

The range of loads for which limit cycles exist was found to be substantial. This is important for the operation of large machinery because such cycles permit the operation at loads much higher than the ones that correspond to the onset of instability of the linearized system. The conditions for the limit cycle deterioration into chaotic orbit are investigated. Analytical expressions have been obtained for the different stability thresholds for the De Laval rotor.

Key Words: *Rotor Dynamics; Steam whirl; Turbomachinery; Rotor stability; Nonlinear systems; Limit cycles*

IN the 1940s, two noncondensing turbines built by the General Electric Company, having very flexible rotors, experienced very violent whirl at high loads (Dimarogonas & Paipetis [1983]). This whirl could not be corrected with balancing and was present only at high loads. An empirical stability criterion, called Torque Deflection Number, resulted from investigations related to those two unstable turbines of General Electric. Thomas [1956, 1958] reported similar problems with AEG turbines and was the first to give a rational explanation supported by a simple analytical model and experiments. Thomas identified the source of the excitation and developed a stability criterion based on a combination of analytical results and experimental calibration. He concluded that the excitation is due to the steam flow through the seal clearances and the stabilizing effects come from the damping forces. He reported also that the problem was corrected, mainly, by decreasing the span and thus raising the critical speed and, sometimes, by bearing changes. Landzberg [1960] used a transfer matrix technique to evaluate the stability of turbine rotors to steam excitation. Alford [1965] reported that modification to the steam path largely eliminated the problem of the General Electric turbines that experienced this type of instability. Both Thomas and Alford agreed that the vibration occurred at frequencies equal to the critical speed of the rotor. Alford, however, stated that variation of the whirl speed in jet engines varied within a wide range, depending on the amplitude and the test conditions.

In the late 1960s the problem came back into attention, and several papers published in Germany dealt with the problem along the same lines with Thomas (Gash [1965]; Kraemer [1968]; Vogel [1970, 1971]). At the same time, large turbines of General Electric (1 GW size) had steam whirl problems and Dimarogonas [1971a, 1971b, 1972] reported on related analytical and experimental investigations.

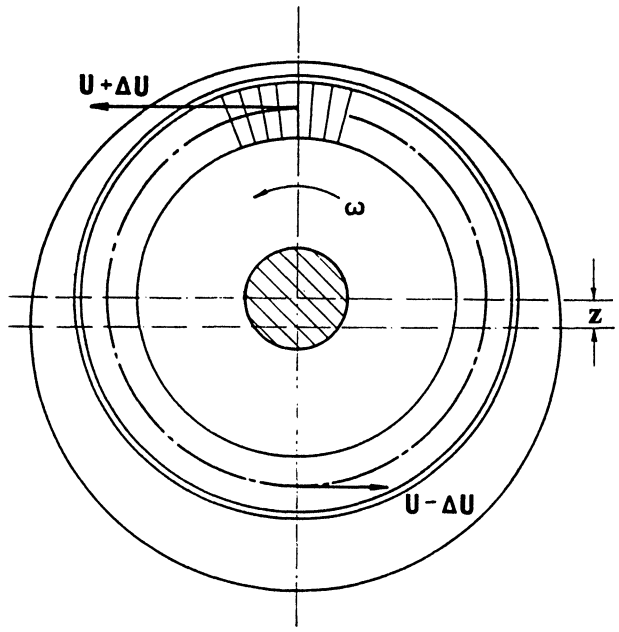

FIGURE 1 Unbalanced peripheral (follower) force due to the rotor displacement in a power stage.

Black [1974] investigated flow induced vibration in high-speed centrifugal pump rotors and instabilities due to local reversed flows at very low flow rates. Shapiro and Colsher [1977] examined the influence of bearings on steam whirl and Pollman *et al.* [1977] and Wright [1977] investigated the excitation mechanisms.

FLUID-INDUCED EXCITATION

Thomas [1956, 1958] was the first who gave a clear identification of one of the main stimuli of steam-whirl, the unbalanced tangential follower-forces due to leakage flow through the seal clearances. In Figure 1 a misaligned stage is shown. We observe that at the area of smaller clearances, there is less leakage, therefore more steam available to produce shaft work. Consequently the peripheral force at this point will be greater than at the area of larger clearances. Assuming that the efficiency of the stage is, in first approximation, a linear function of the clearance, one can conclude that the change in the tangential force $2\Delta U$ is proportional to the rotor deflection z. The coefficient of proportionality k_{st} will be called flow force gradient, $k_{st} = \partial U/\partial z$.

The same situation exists for flow through the shaft seals. Therefore, the flow force gradient k_{st} consists of two terms and it is (Thomas [1956])

$$\partial U/\partial z = (T/hd_m)[\xi_s(d_n/d_m)^2\phi\sqrt{2gH}/(C_2 \sin a_2\sqrt{Z}) + \xi_b(1 + h/d_m)] \quad (1)$$

where U is the peripheral force of the stage $= T/(d_m/2)$, T the stage torque, z the shaft deflection, h the nozzle height, d_n the shaft diameter, d_m the pitch diameter of stage, H the adiabatic drop of stage, ϕ the velocity coefficient, C_2 the absolute exit velocity, a_2 the exit angle, Z the number of seal teeth, g the acceleration of gravity.

One can recognize immediately the two terms in the bracket as representing the gradients due to leakage at shaft and blade seal, respectively. The two coefficients ξ_s and ξ_b are calibration constants determined experimentally. They account for secondary factors, such as circumferential flow, pressure-equalizing holes and other effects on efficiency. Thomas determined them experimentally and suggested values $\xi_s = 1.6 \cdots 2$ and $\xi_b = 0.6 \cdots 1.5$. Therefore, in his work, other mechanisms for follower-force gradients have also been taken into account in these constants. This flow-induced Thomas follower-force gradient has been called by some authors, erroneously, "Alford's Force." Dimarogonas [1971] has integrated the local effect around the periphery of the stage using a more accurate expression for the leakage due to Pfleiderer [1952], to obtain

$$\partial U/\partial z = (T/hd_m)[\xi_s(d_n/d_m)^2\phi\sqrt{2gH(1-r)} /(C_2 \sin a_2\sqrt{Z}) + \xi_b(d_c/d_m)^2\psi\sqrt{2rgH} /(w_1 \sin b_2\sqrt{Z_c})] \quad (2)$$

where d_c the outer diameter of the stage $= h + d_m$, r is the reaction of the stage, Z_c the number of teeth over the blade cover, w_1, b_2 the entrance velocity and angle at the stage. Dimarogonas [1971] used proprietary General Electric leakage formulas that account accurately for the leakage flow. Equation [2] could be used here if the design information is not available. In general, however, the gradient in eq. [2] is available at the design stage for every turbine design in the form of the ratio $q = \Delta E_{loss}/\Delta c$, where ΔE_{loss} is the loss of the stage efficiency and Δc the clearance change (increase). If N is the power of the stage, the loss is $N\Delta E_{loss}$. The additional torque is $-N\Delta E_{loss}/\omega$ and the corresponding additional peripheral force is $-2N\Delta E_{loss}/\omega(d_m + h)$. Over an angle $d\phi$, this peripheral force is, Figure 2,

$$dP = -N\Delta E_{loss}\, d\phi/\omega\pi(d_m + h). \quad (3)$$

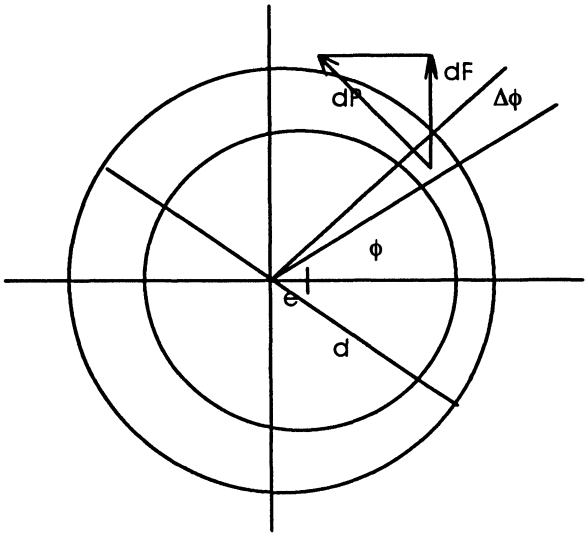

FIGURE 2 Integration of the local follower force.

The lateral force is

$$dF = dU\cos\phi = -N\Delta E_{\text{loss}}\cos\phi d\phi/\omega\pi(d_m + h). \tag{4}$$

If c is the clearance, $\Delta c = -e\cos\phi$, where e is the stage eccentricity. Therefore,

$$\begin{aligned} dF &= -N\Delta E_{\text{loss}}\cos\phi d\phi/\omega\pi(d_m + h) \\ &= -Nq\Delta c\cos\phi d\phi/\omega\pi(d_m + h) \\ &= Nqe\cos^2\phi d\phi/\omega\pi(d_m + h). \end{aligned} \tag{5}$$

Integrating around the stage, for $\phi = 0$ to 2π,

$$F = Nqe/\omega(d_m + h). \tag{6}$$

The Thomas follower force gradient is then,

$$\partial U/\partial z = F/e = Nq/\omega(d_m + h) = Tq/(d_m + h). \tag{7}$$

This formula should be used for design calculations (Dimarogonas [1971a, 1972]).

Alford [1965] proposed another model for the axial flow around the blade cover, assuming no effects of circumferential flow and considering variation of static pressure in a two-teeth blade seal due to the motion of the shaft. This phenomenon appears to contribute to the problem only when the upstream tooth clearance is greater than the downstream one and does not seem to have a considerable effect in practical situations.

Circumferential flow in the cavity of the shaft seals or at the stage seals might generate substantial follower-force gradients. Dimarogonas [1971b] computed the pressure distribution in the seal cavities due to the circumferential flows and found that for large steam turbine stages the magnitude of the follower-force gradient due to the circumferential flow is small as compared with the Thomas follower-force gradient. The circumferential flow becomes more important as the machine speed increases and the machine size decreases.

Equation [7] can be used to find the Thomas follower-force gradient since its ingredients are inherent in any turbine design system. Most probably due to the proprietary nature of these systems, several authors have reported recently extensive experimental and numerical investigations on the Thomas follower-force gradient, for example, Bencket [1980], Childs *et al.* [1977–1993], Iwatsubo & Yang [1988]; Nelson [1984–1987]; Vance [1984, 1988]; Nordman *et al.* [1987–1988]; Wright [1977, 1984]; Wyssmann *et al.* [1984, 1987], Baumgartner [1987], Dietzen & Nordmann [1987], Diewald & Nordmann [1987]. For design purposes, however, the design systems that are based on long experience and research should be used, if at all possible.

BEARING NONLINEARITY

Even up to the present day, most of the rotor-bearing stability analyses are based on the first method of Liapounov, that is, the linearization of the equations of motion about the equilibrium position. Since the bearings are the major source of nonlinearity, this linearization involves expressing the bearing forces by means of the so-called 'bearing dynamic coefficients'. These coefficients are the gradients of the oil-film forces along the different coordinates, $K_{ij} = \partial F_i/\partial X_j$, $C_{ij} = \partial F_i/\partial \dot{X}_j$ where F_i is the force along the i-direction, X_j is the displacement along the j-direction, $\dot{X}_j$ is the velocity along the j-direction. The most simplistic approach involves isotropic bearing characteristics. In this formulation only one stiffness coefficient exists without cross-coupled terms, and the rotor-bearing system response produces only circular orbits. The utility of the results using this oversimplified model is rather limited. A further step in the isotropic bearing model, is to consider the cross-coupled bearing coefficient. Here the orbits are still circular but instability is possible because cross-coupling results in destabilizing follower forces, similar in effect to the steam-force gradient follower forces. By extending the bearing model even further to nonisotropic bearings we arrive at four different stiffness coefficients and four linear damping bearing coefficients, that permit representation of heavy-loaded rotors operating eccentrically in respect to the concen-

tric journal-bearing position. There are numerous bearing tables in the literature, such as by Lund [1965], Nicholas *et al.* [1979], or Orcutt [1965] and linear coefficients (Lund [1965], Orcutt [1965]) with the effect of the oil inertia forces. Tilting-pad bearings have been used in cases that follower forces from the steam flow tend to result in instability. The reason is that tilting-pad bearings have no cross-coupling (follower) force gradient that adds to the steam-flow Thomas follower-force gradients. For such bearings (Lund [1965]) the assembly method is used, that is, evaluating the overall bearing force based on the response of the individual pads and on their relative location. Due to several mechanisms such as oil film rotation, cavitation, and pad critical mass, titling-pad bearings might exhibit follower, cross-coupling forces at high speeds (Nicholas [1978–1979; Lund [1965]).

Using linearized bearing coefficients results in a linear mathematical model for the system. Its stability analysis is well understood now and used very extensively Ehrich [1972, 1988], Ehrich & Childs [1984], Elrod *et al.* [1989, 1990], Flack & Zuck [1987], Fowlie & Miles [1975], Holmes & Sykes [1989], Kim & Childs [1987], Kirk [1988], Kirk & Miller [1979], Kirk & Reddy [1988], Pollman *et al.* [1977], Rajakumar & Sisto [1990], Ruhl & Booker [1971], Sharrer [1988], Sharrer & Nelson [1991], Tam *et al.* [1988], Wang *et al.* [1988, 1989], Weiser and Nordman [1989]. Experience has shown, however (Dimarogonas [1971]), that a system can operate with small stable limit cycles way beyond the onset of instability of the linearized system within acceptable levels of limit cycle amplitudes. This renders the nonlinear analysis essential. The possibility of such stable limit cycles has been demonstrated (Dimarogonas [1975]; Dimarogonas & Paipetis [1983]).

The computation of the linearized bearing properties for fixed-pad bearings (elliptical bearings are the ones used for low-pressure turbine rotors) is well known (Lund [1965]; Dimarogonas [1988]). It uses finite element or finite difference solutions of the lubrication equation with a 3×3 grid of points enclosing the equilibrium position or by perturbation solution of the differential equations. Next, the nonlinear oil forces in the neighborhood of the equilibrium point (an extended grid that allows the computation of the higher derivatives) are evaluated and a finite difference scheme is used for the computation of higher derivatives. Alternatively, higher order perturbations can be used. For example, up to the 3rd order derivatives are retained, 18 linear and nonlinear bearing stiffness coefficients can be computed moving the journal within a zone composed of 25 sub-grid points (the distance between these points being a small fraction of the bearing operating eccentricity) about the equilibrium point. Finally, the oil-film bearing forces are expressed as a Taylor expansion about the equilibrium position, with all the high-order terms up to the third-order power plus a remainder as follows:

$$F_x(X, Y) = F_x(0, 0) + \Sigma_i K_{xi} i + [\Sigma_i \Sigma_j \varepsilon_{ij} S_{xij} ij]/2! + [\Sigma_i \Sigma_j \Sigma_k \rho_{ij} \rho_{ik} \rho_{jk} S_{xijk} ijk]/3! + R_x(4) \tag{9}$$

$$F_y(X, Y) = F_y(0, 0) + \Sigma_i K_{yi} i + [\Sigma_i \Sigma_j \varepsilon_{ij} S_{yij} ij]/2! + [\Sigma_i \Sigma_j \Sigma_k \rho_{ij} \rho_{ik} \rho_{jk} S_{yijk} ijk]/3! + R_y(4) \tag{10}$$

where S_{xij} and S_{yij} are the second bearing coefficients $(\partial^2 F/\Delta ij)$, ε_{ij}, ρ_{ij} are numerical parameters for the Taylor expansion, S_{xijk}, S_{yijk} are the third-order bearing coefficients $(\partial^3 F/\partial ijk)$, and $i, j, k = X$ or Y.

In this way we closely represent the journal-bearing behavior within a certain range (not just about a point, as it is generally done). Moreover, we can expect a much better bearing force approximation for journal displacements within the grid mesh zone (Dimarogonas [1993]).

A large number of utility industry turbines that display steam-whirl instability are mounted on tilting-pad bearings. These bearings have a significantly different dynamic behavior from the typical fixed pad bearing; the basic difference is their lower, practically negligible first-order cross-coupling stiffnesses and damping coefficients, which makes them resistant to oil whip phenomena. Another important characteristic of tilting-pad bearings is that, multipad tilting-pad bearings with load-on-pad tend to exhibit more asymmetric characteristics along the vertical and horizontal planes as compared with load-between-pads tilting-pad bearings. The latter tend to be isotropic, due to the symmetry and this is an important property in simplifying the analysis. Moreover, usually they exhibit better stability behavior and they are widely used.

Andritsos and Dimarogonas ([1980]; Dimarogonas and Andritsos [1986]) have noticed that if the inertia of the pad is neglected, as compared with the rotor inertia, the force between the rotor and the pad has the direction of the line connecting the pad pivot and the rotor center and they depend only on the oil film thickness at the pivot point. They subsequently developed an experimental procedure for the determination of the bearing forces by means of nonlinear stiffness and damping pad functions. These functions describe the pad bearing reaction for any location of the journal. For instance, at any given pad, the pad reaction force can be expressed as the addition of two terms. One

of these terms accounts for the static wedge force W_p, and the second one accounts for the squeeze film effect F_p as follows:

$$F = W_p + F_p = f(H_p) + B_p dH_p/dt \qquad (11)$$

where

$W_p = 1/S_{ow}$,
$S_o = \xi nDL(R/C_m)^2/W_p$, the Sommerfeld Number for the static force,
$B_p = 1/S_{ob}$
$S_{ob} = \xi nDL(RC_m)^2/(nC_mB_p)$, the Sommerfeld Number for the damping force,
$W_p = f(H_p) = a + bE_p + cE_p^m/(1 - E_p^2)^n$, dimensionless wedge force of pad,
$B_p = a_k + b_kE_p + c_kE_pm_k/(1 - E_p^2)_k^n$, dimensionless squeeze effect force of pad,
$E_p = 1 - H_p/C_m$, the eccentricity ratio at the pivot point,
H_p is the oil-film thickness at the pivot point,
C_m is the machined radial clearance of pad,
n is the speed of rotation, Hz,
$D = 2R$ is the journal diameter,
L is the journal length,
ξ is the dynamic viscosity,
$a, b, c, m, n, a_k, b_k, c_k, m_k, n_k$ are curve fitting parameters determined experimentally or numerically.

The performance of the complete bearing is then computed from an assembly of the individual pad functions. This yields a complete nonlinear description of the bearing forces regardless of journal distance from the equilibrium position. The pad function parameters a, b, c, m, n for the stiffness function and a_k, b_k, c_k, m_k, n_k for the damping functions were found experimentally for a variety of pads and tabulated in Andritsos and Dimarogonas [1980] and Dimarogonas and Andritsos [1986], respectively.

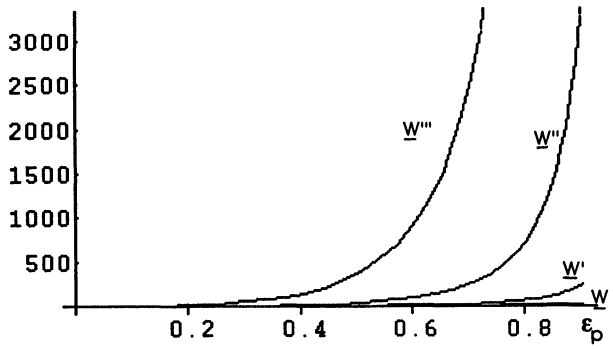

FIGURE 3 Derivatives of the dimensionless pad force W versus journal eccentricity E_p.

The selection of the four-pad bearings-load between pads in this work, beyond reflecting current design practices of turbine manufactures, facilitates further analysis. Since the bearings are isotropic, they can be described with fewer parameters. Indeed, one might notice that since all directions are equivalent, stiffness and damping can be evaluated in the direction of a single pad. In this case, the other pads do not have a significant contribution and, in the absence of cross-coupling terms,

$$K_x = K_y = dW_p/dE_p$$
$$= \left[b + cmE_p^{m-1}(1 - E_p^2)^{-n} + 2cnE_p^{m+1}(1 - E_p^2)^{-n-1}\right]/C_m \qquad (12)$$

$$K_{2x} = K_{2y} = d^2W_p/dE_p^2$$
$$= \left[cd^2E_p^m/(1 - E_p^2)^n/dE_p^2\right]/C_m^2 \qquad (13)$$

$$K_{3x} = K_{3y} = d^3W_p/dE_p^3$$
$$= \left[cd^3E_p^m/(1 - E_p^3)^n/dE_p^3\right]/C_m^3 \qquad (14)$$

One can observe that the stiffening effect, the nonlinear spring-like bearing behavior, is an odd function, therefore only the third derivative is of interest for a simplified analytical model. The three derivatives of the static pad load W_p are shown in Figure 3.

THE DE LAVAL ROTOR MODEL

The problem of steam whirl is one of the technological limitations that slowed down and finally halted the development of power-generating turbomachinery substantially above 1 GW. Due to steam flow, self-excited vibrations develop at high loads, above the onset of instability of the linearized system, in the form of stable limit cycles that, at even higher loads, deteriorate to chaotic vibration.

In the realm of a linear system, there is already a substantial body of literature (Thomas [1956, 1958], Landzberg [1960], Alford [1965], Dimarogonas [1971, 1972]. It has been observed in operation, however, that the onset of instability of the linear system, that appears as the point where elliptical orbits start developing at the rotor natural frequency at running speed, is at substantially lower load than the one the mechine can sustain within acceptable vibration levels due to the limit cycles developing because of the bearing nonlinearity.

Dimarogonas [1987] has demonstrated the existence of

limit cycles due to fluid excitation in the form of follower forces in rigid rotors on nonlinear pad bearings.

To study the problem of the effect of rotor flexibility, a de Laval rotor (Föppl [1895]), called erroneously "Jeffcott Rotor" by some authors, is considered with

a) Identical isotropic nonlinear bearings.
b) Symmetric rotor with single mid-span disc.
c) Negligible bearing cross-coupled damping and stiffness.

A complex plane is used to represent the lateral forces as in Figure 4. O_b is the location of the shaft geometric center at the bearing location and O_s the shaft geometric center at the mid-span. δ is the deflection at the bearing and z the deflection of the disk at the mid-span, while the forces acting at the different points are as shown. The origin of the coordinate system is placed at the equilibrium point of the system. Newton's second law applied to the disk center of mass gives and force equilibrium at the journal give

$$\begin{aligned} mz'' &= -k(z-\delta) - ik_{st}z \\ k(z-\delta) &= K\delta + C\delta' + K_3|\delta|^2\delta \end{aligned} \tag{15}$$

where m is the mass of the disk, k the stiffness of the shaft assumed simply supported at the bearings, K and C the stiffness and damping constants, respectively, of the two bearings, assumed isotropic and identical, with the disk at the mid-span, K_3 the nonlinear bearing coefficient of order 3, $k_{st} = \partial U/\partial z$ the follower flow force gradient (Thomas coefficient). Higher-order bearing coefficients have been introduced by Dimarogonas [1971, 1976], Dimarogonas and Paipetis [1983] and Andritsos and Dimarogonas [1980, 1986].

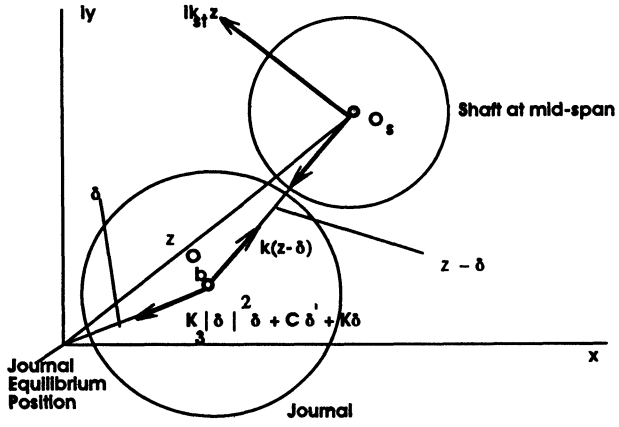

FIGURE 4 Rotor-bearing system geometry of motion and reaction forces in a de Laval rotor.

The third-order approximation was selected in view of the odd character of the additional nonlinear forces that are known to have a hardening effect in a journal bearing. The higher order terms in a Taylor expansion of the bearing forces about the point of equilibrium were obtained using RODYNA (Clayton Labs [1989]) and a grid of finite differences about the point of equilibrium.

Eliminating δ in eqs. [15] yields

$$\begin{aligned} &(Cm/k)z''' + m(1+K/k)z'' + C(1+ik_{st}/k)z' \\ &\quad + [K + ik_{st}(1+K/k)]z \\ &\quad = -k_3|[z + (mz'' + ik_{st}z)/k]|^2 \\ &\quad \times [z + (mz'' + ik_{st}z)/k] \end{aligned} \tag{16}$$

The linearized equation is

$$\begin{aligned} &(Cm/k)z''' + m(1+K/k)z'' + C(1+ik_{st}/k)z' \\ &\quad + [K + ik_{st}(1+K/k)]z = 0 \end{aligned} \tag{17}$$

To investigate the feasibility of harmonic response, the solution is set in the form $z = z_0 e^{pt}$ to yield the characteristic equation

$$\begin{aligned} &(Cm/k)p^3 + m(1+K/k)p^2 + [C + iC(k_{st}/k)]p \\ &\quad + [K + ik_{st}(1+K/k)] = 0 \end{aligned} \tag{18}$$

Dividing equation 16 by $C_m k$, where C_m is the bearing clearance, and using the dimensionless time $\tau = \omega t$ and amplitude $\zeta = z/C_m$ we obtain

$$\begin{aligned} &\eta\lambda^2\zeta''' + \lambda^2(\alpha+1)\zeta'' + \eta[1 - i\beta]\zeta' \\ &\quad + [\alpha - i\beta(\alpha+1)]\zeta = -\varepsilon\zeta|\zeta|^3 \end{aligned} \tag{19}$$

where a prime denotes derivative in respect to τ,

$$\varepsilon = \gamma[1 + \lambda^2\zeta''/\zeta - i\beta]^3 \tag{20}$$

is assumed to be small and ω is the frequency of rotation, ω_n is the natural frequency of the shaft on rigid bearings $= (k/m)^{1/2}$ and the nondimensional governing parameters are,

$\eta = \alpha\omega C/K$, damping parameter,

$\alpha = K/k$, bearing over shaft stiffness ratio,

$\lambda = \omega/\omega_n$, operating frequency ratio,

$\beta = k_{st}/k$, follower flow force gradient ratio,

$\gamma = (K_3/k)C_m^2$, 3rd-order bearing nonlinearity ratio.

THE LIMIT CYCLE

For some value of the Thomas follower-force gradient $\beta = \beta_L$, that we shall find later, the characteristic equation [18] will have a solution with a positive real part and this will be the linear onset of instability. If the load increases and β exceeds this value then the amplitude would not increase beyond bound as the linear system theory predicts. Instead, nonlinearity will confine the amplitude within a certain orbit, a closed cycle. To investigate the limit cycle, a quasi-harmonic response is assumed, in tune with the experimentally observed elliptical orbits associated with such cycles, at least for small loads. To this end, the solution of the linearized equation is sought first in the form,

$$\zeta = \zeta_0 e^{ip\tau} \tag{21}$$

where $p = p_r + ip_i$.

Substituting eq. [21] into eq. [19] and dropping the nonlinear term,

$$\eta\lambda^2\left[\left(3p_r^2 p_i - p_i^3\right) - i\left(p_r^3 - 3p_r p_i^2\right)\right] - \lambda^2(\alpha+1) \times \left[\left(p_r^2 - p_i^2\right) - 2ip_r p_i\right] + \lambda[-p_i + ip_r] + \lambda\beta[p_r + ip_i] + [\alpha - i\beta(\alpha+1)] = 0 \tag{22}$$

Separating the real and imaginary parts, we obtain, respectively:

$$\eta\lambda^2\left[\left(3p_r^2 p_i - p_i^3\right)\right] - \lambda^2(\alpha+1) \times \left[\left(p_r^2 - p_i^2\right) - \lambda p_i + \lambda\beta p_r + \alpha\right] = 0 \tag{23}$$

$$-\eta\lambda^2\left[\left(p_r^3 - 3p_r p_i^2\right)\right] - 2\lambda^2(\alpha+1) \times p_r p_i + \lambda p_r + \lambda\beta p_i - \beta(\alpha+1) = 0 \tag{24}$$

For a given $\beta < \beta_L$, i.e., β smaller than the linear onset of instability, solving eqs. [23] and [24] simultaneously will yield $p_i > 0$. This indicates that there is transient vibration, which eventually will die out and the system is stable.

To obtain the linear threshold we set $p_i = 0$, in both equations [23] and [24] and solve them simultaneously for p_r and β_L. We obtain by symbolic manipulation, using Mathematica,*

$$p_r^2 = 1/(2\eta^2\lambda^2)[\eta^2 - \lambda^2(\alpha+1)^2 + \left[\left\{\lambda^2(\alpha+1)^2 - 1\eta^2\right\}^2 + 4\lambda^2\eta^2\alpha(\alpha+1)\right]^{1/2}] \tag{25}$$

$$\beta_L = p_r\left(\eta - p_r^2\right)/(\alpha+1)$$

*Wolfram, S. 1991. Mathematica. Reading, Mass: Addison Wesley.

THE NONLINEAR APPROXIMATION

Using eqs. [25] with $p_i = 0$ and solving equation 19 for ζ, we obtain the expression for ζ^2, that denotes the displacement of the rotor from the trivial static equilibrium position,

$$\zeta^2 = \left\{\left[\lambda^2(\alpha+1)p_r^2 - \eta\beta p_r - \alpha\right] + i\left[\eta p_r\left(\lambda^2 p_r^2 - 1\right) + \beta(\alpha+1)\right]\right\}/\gamma \tag{26}$$

where p_r could approximately be substituted from eqs. [25] but here is used implicitly in order to simplify the expression. In tune with the experimental observation that at the onset of instability the frequency of the whirl is ω_n and thus $\lambda p_r = 1$,

$$\zeta^2 = [(1 - \eta\beta p_r) + i\beta(\alpha+1)]/\gamma \tag{27}$$

We notice that at the limit cycle onset, the square of the amplitude is practically proportional to the steam gradient and, approximately, inversely proportional to the third-order bearing coefficient ratio γ; a result in tune with experimental observations. In the absence of damping ($\eta = 0$), the amplitude is practically directly proportional to the excitation parameter β. The (linear) onset of instability load parameter β_L marks the first overall system bifurcation.

When using any of these analytical expressions, we must observe the following limitations:

a) Both β and η have to be small, with the whirl frequency ratio p_r given by equations 25. This is not a severe complication because we know that the whirl frequency near the onset of instability coincides with the rotor natural frequency at running speed.

b) we cannot assume $\beta = 0$ and $\eta = 0$ at the same time, since β must be $>\beta_L$ in order to make physical sense; i.e., machine operating in limit cycle region, beyond the linear stability onset. The larger the η, the larger the β_L will be. On the other hand, it is possible to assume $\eta \to 0$.

The dependence of amplitude on the follower-force parameter β and the bearing damping parameter η is shown in Figure 5. It is observed that there is an optimum range of the bearing damping parameter η between 15 and 30 where the excitation parameter β and the load have maxima for the same vibration amplitude level ζ.

A trivial solution (both load parameters, β and ξ being zero) of eq. [19] will be

$$\lambda^2 p_r^2 = 1 \tag{28}$$

which is equivalent to the resonant response solution.

Following the same line of reasoning as for the derivation of the amplitude ζ, the expression for the amplitude at the bearing δ is

$$\delta = (m/k)z'' + [1 - i(k_{st}/k)]z = \mathrm{Re}(\delta) + i\mathrm{Im}(\delta) \quad (29)$$

which after normalization and substitution of ζ from eq. [27] yields an approximate expression for the complex dimensionless bearing amplitude δ_b', and dimensionless bearing velocity δ_b', respectively,

$$\delta_b = [-p_r^2\lambda^2 + 1 - i\beta]\zeta = \mathrm{Re}(\delta_b) + i\mathrm{Im}(\delta_b) \quad (30)$$

$$\delta_b' = \{\beta + i[1 - p_r^2\lambda^2]\}p_r\zeta \quad (31)$$

We express, F_b, the nonlinear force at the bearing in dimensionless form,

$$\begin{aligned} F_b &= -\eta\delta_b' - (1+\alpha)\delta_b - \gamma\delta_b^3 + \zeta \\ &= [-\eta\mathrm{Re}(\delta_b') - (\alpha+1)\mathrm{Re}(\delta) - \gamma(\mathrm{Re}(\delta)^3 \\ &\quad - 3\mathrm{Re}(\delta_b)\mathrm{Im}(\delta_b)^2) + \mathrm{Re}(\zeta)] + i[-\eta\,\mathrm{Im}(\delta_b') \\ &\quad - (\alpha+1)\mathrm{Im}(\delta_b) - \gamma(-\mathrm{Im}(\delta_b)^3 \\ &\quad + 3\,\mathrm{Re}(\delta_b)^2\mathrm{Im}(\delta_b)) + \mathrm{Im}(\zeta)] \\ &= \mathrm{Re}(f_b) + i\mathrm{Im}(f_b) \end{aligned} \quad (32)$$

where δ_b, δ_b' are given by equations [30] and [31].

In the same way we can obtain the nonlinear force at the rotor.

NONTRIVIAL EQUILIBRIA

The above analytical model, equation [19], renders three static equilibrium points. The one of them, as well as the most important one, is the zero equilibrium point. The other two fall within a same distance from the origin, differing only in their phase angle. The nontrivial equilibrium points, ζ_{eq}, seem to play an important role.

For highly loaded bearings with relatively small Sommerfeld number, the nontrivial equilibrium positions fall quite close to the origin. Under this condition, only a moderate magnitude perturbation (initial conditions) is able to make the system come close to the nontrivial equilibrium and thus produce a chaotic response, provided that such perturbation is sufficiently close to the nontrivial equilibrium point. Moreover, even for the case of sufficiently small initial conditions, when the load parameter β is large enough as to have an orbit δ_b of approximately the same magnitude as the nontrivial equilibrium points $|\zeta_{eq}|$, an unstable limit cycle also occurs. The reason been that for such β, these equilibrium points are already unstable nodes, therefore they act as repeller nodes.

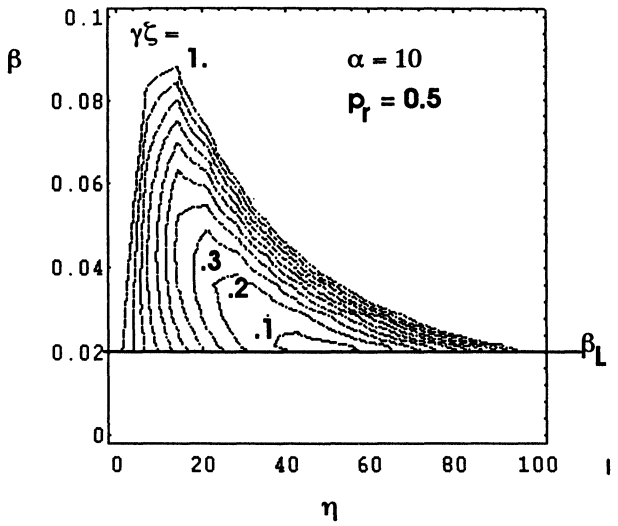

FIGURE 5 Dimensionless amplitude ζ of the de Laval rotor as function of the flow-force gradient parameter β and the bearing damping parameter η.

They possess either a stable or unstable limit cycle of their own, which interacts with the limit cycle stemming from the trivial position. This causes the system to experience further bifurcations of its behavior. The expression for the nontrivial equilibrium positions is,

$$\zeta_{eq} = [-\alpha + i\beta(\alpha+1)]^{1/2}/[\gamma(1 - 3\beta^2) + i\beta(\beta^2 - 3)]^{1/2} \quad (33)$$

Figures 5, 6, and 7 show the rotor response for progressively higher loads and proportionally higher excitation coefficients β. They have been obtained numerically with POINCARE, a simulation code (Dimarogonas [1993]). Nonlinear bearing properties were obtained with RODYNA, a finite element rotor-bearing code [Clayton Labs [1989]).

Figure 6 shows an elliptic, stable limit cycle at load slightly above the linear threshold. Figure 7 shows a stable limit cycle at load significantly above the linear threshold. The ellipticity is lost, higher harmonics appear and the repelling effect of the nonstable equilibria is apparent. Figure 8 shows a Poincare Map of the chaotic response to which the unstable limit cycle degenerates at load far above the linear threshold.

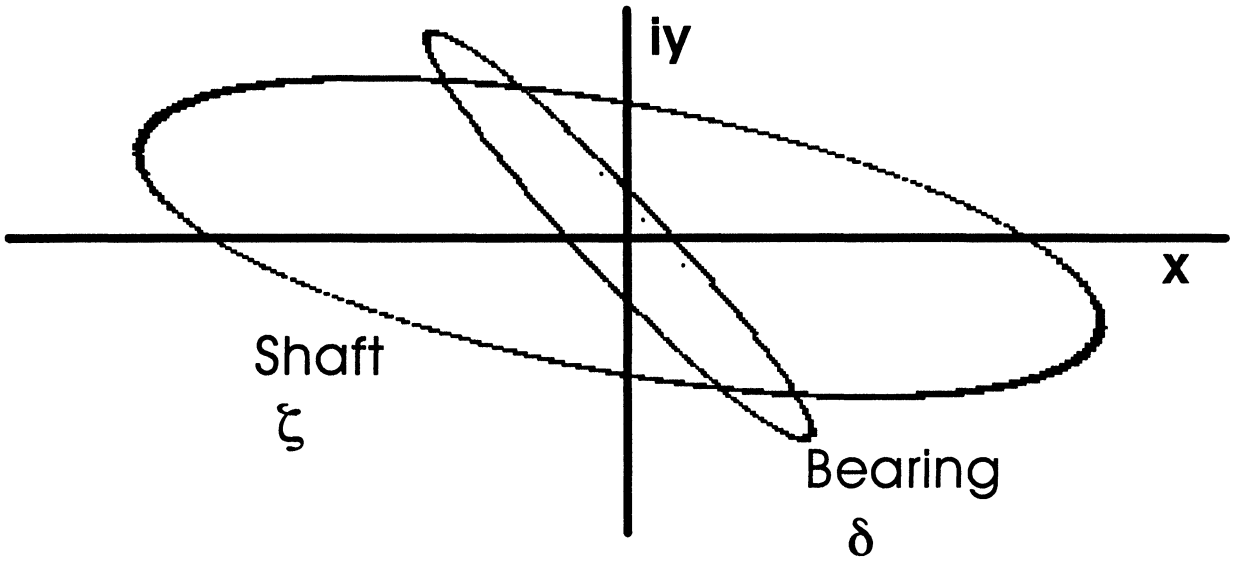

Parameters:	$\alpha = 2$	$\lambda = 1.5$	$\eta = 5$	$\gamma = 100$	$\beta = 0.33$

FIGURE 6 Stable limit cycle of a de Laval rotor for relatively small β.

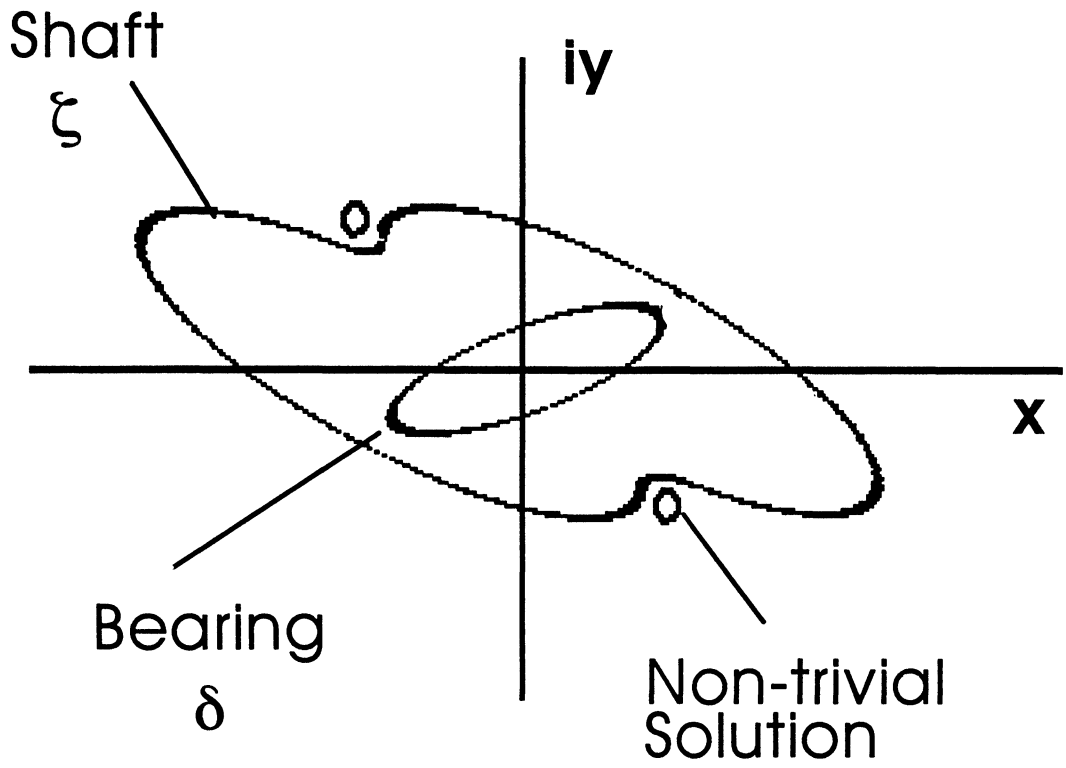

Parameters:	$\alpha = 1.82$	$\lambda = 1.72$	$\eta = 2.5$	$\gamma = 200$	$\beta = 0.14$

FIGURE 7 Stable limit cycle of a de Laval rotor for large β.

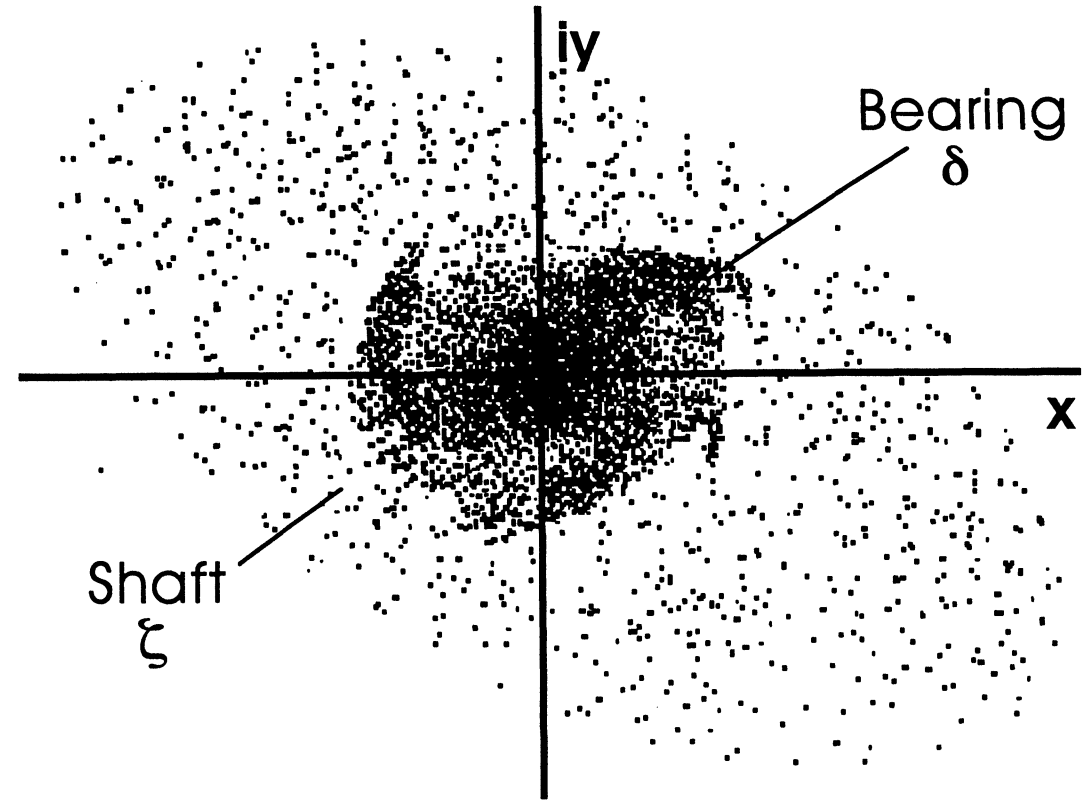

Parameters:	α = 3.18	λ = 1.5	η = 1.5	γ = 400	β = 0.33

FIGURE 8 Chaotic vibration of a de Laval rotor for very large β.

STABILITY OF THE LIMIT CYCLE

Within the region beyond the linear onset, several bifurcations in the behavior of the system continue to occur. Beyond the initial bifurcation at the linear onset β_L, another one occurs within the limit cycle range. The complexity of the limit cycle increases with each bifurcation, until instability of the cycle is reached.

There are two alternatives for the classification of these bifurcation points. The first alternative concentrates its analysis using expressions related with the zero (trivial) equilibrium position. On the other hand, the second alternative for the classification of the bifurcation points takes into account the other two equilibrium points, regarding them as points which have a zone of influence surrounding them (Thompson and Steward [1986], Awrejcewitz and Mrozowski [1989]). The interaction of the limit cycle (stemming from the origin) and these zones of influence, yields a progressive number of bifurcations in the response behavior, the more extensive this overlapping, the more interaction and bifurcations that will take place.

The first classification alternative will define their bifurcations as follows. The first bifurcation in the nonlinear region takes place when the whirl load is high enough as to raise the dimensionless force at the bearing to a value of approximately 0.05 and it is denoted by $\beta_{(Fb=.05)}$. Therefore this bifurcation denotes the end of the elliptic orbit with a unique frequency.

The second nonlinear bifurcation, β_{b1} denotes the occurrence of either the real or the imaginary part of the predicted rotor amplitude becoming zero. Therefore β_{b1} denotes the upper bound of the stable periodic limit cycle.

The second alternative to classify the bifurcation points is as follows. The nontrivial equilibrium points will loose their linear stability β_{Leq} well before the zero equilibrium point; i.e., $\beta_{\text{Leq}} < \beta_L$. Under this circumstance, we can assume that another elliptical limit cycle surrounds each of these nontrivial equilibria. Both limit cycle amplitudes ζ_{eq}, as well as their whirl frequencies p_{req}, can be

computed by perturbing eq. [19] around these nontrivial equilibria. When two amplitudes, emanating from different directions, touch each other, i.e., $|\zeta| = |\zeta_{eq}|$, the first nonlinear bifurcation β_{eq1}, will occur. Also in this criterion, β_{eq1} denotes the end of a unique whirl frequency and elliptical limit cycle orbit.

Since it is expected that ζ_{eq} will increase at a higher rate than ζ, the second bifurcation β_{eq2} will take place when $|\zeta_{eq}| = |\zeta_{0eq}|$, that is to say, when the influence zone surrounding a nontrivial equilibrium point becomes equal to its distance to the origin.

This results in an extensive overlapping of the attracting limit cycles zones and therefore it is expected that this condition approximately marks the system's unstable limit cycle bifurcation. That is to say, for most cases a β beyond β_{eq2} will yield an unstable aperiodic limit cycle ζ, but with perhaps a still bounded amplitude orbit. For practical purposes, β_{eq2} can be considered the lower bound for the stable and periodic limit cycle.

Futhermore and in a similar manner, when $|\zeta| = |\zeta_{0eq}|$, the third nonlinear bifurcation β_{eq3} will occur. For any $\beta > \beta_{eq3}$, the system will certainly yield an aperiodic unstable limit cycle.

Moreover, the unstable limit cycle may contain superharmonic whirl frequency components with infinite amplitude, as it is observed during the numerical simulation. Therefore it can be safely expected that β_{eq3} can definitely by considered the upper bound for the stable limit cycle.

LOAD STABILITY CRITERION

The development of a single criterion to predict instability of turborotors due to steam whirl has been the subject of numerous investigations. Alford [1965] reported that General Electric alleviated the instability problems they experienced in the 1940s developed a load-stability criterion. They found that the static deflection of a rotor due to the power generating peripheral force at rated load, assumed acting at mid-span, was correlating with the experience with turbine rotors that had experienced steam whirl. This criterion, *Torque Deflection Number,* in terms of the design parameters, was be expressed as:

$$\mathrm{TDN} = N y_{\max}/d_m W n \tag{34}$$

where $y_{\max}$ the maximum deflection defined above, N the rated power of the rotor, d_m the average blade pitch diameter, W the rotor weight and n the speed of rotation (Hz). In terms of the parameters used here,

$$\mathrm{TDN} = 2\pi T/d_m k \tag{35}$$

The good correlation of this criterion was merely coincidental and had no rational basis since it does not include the bearing effects at all. However, it dominated turbomachinery design for a long time.

Thomas proposed a more rational approach: the ratio S/D of the whirl inducing fluid forces S to the damping forces D has to be < 1 for stability. In terms of the design parameters used here,

$$\mathrm{Th} = T/m\omega_k^2\theta S < 1 \tag{36}$$

where T is the rotor torque, ω_k is the rotor critical speed, θ is the logarithmic decrement ω denotes the running speed, $S = hd_m/\pi\mu$, $\mu = \xi_S(d_n/d_m)^2\phi\sqrt{(2gH)}/(C_2 \sin a_2\sqrt{Z}) + \xi_b(1 + h/d_m)$, equation [1]. Therefore

$$\mathrm{Th} = \pi\mu T/k\theta h d_m < 1 \tag{37}$$

Although Thomas interpreted the damping as rotor internal damping, he measured it experimentally on turbine rotors and therefore is in effect the bearing damping and this renders the Thomas criterion rational.

The relation of Th and TDN is, from eqs. [22] and [23],

$$\mathrm{Th} = \mathrm{TDN}(\mu/2\theta h) < 1 \tag{38}$$

For the θ, Thomas reported measured values of 0.05 for critical speed below 1/2 rated speed, 0.1 otherwise. It can be seen from eq. [35] that the TDN criterion does not include the effect of damping and the geometry of the leakage path.

There are factors still missing in the Thomas criterion. The relation of the rotor flexibility to the bearing flexibility is of paramount importance. The fluid forces are functions of the absolute rotor motion, the bearing reactions depend on the absolute journal motions, whose relation to the rotor motion is determined by the relation of rotor and bearing flexibility.

A rational load stability criterion can be found from the linear threshold of instability, eq. (25),

$$p_r(\eta - p_r^2)/(\alpha + 1)\beta_L > 1 \tag{39}$$

Experimental observations (Dimarogonas [1971a, 1972]) showed that the whirl frequency was near the rotor natural frequency at running speed, rendering $p_r \approx \omega_n/\omega$ and $\lambda p_r \approx 1$. Equation [39] gives the load stability criterion, assuming that $\alpha = K/k \gg 1$

$$\mathrm{LSC} = K k_{st}(\omega/\omega_n)/k^2(\omega C/k - \omega/\omega_n) < 1 \tag{40}$$

Substituting the value of k_{st} from eq. [2]

$$\mathrm{LSC} = T\mu K(\omega/\omega_n)/[h d_m k^2(\omega C/k - \omega_n/\omega)] < 1 \tag{41}$$

where

$$\mu = [\xi_s (d_n/d_m)^2 \phi \sqrt{[2gH(1-r)]}/(C_2 \sin a_2 \sqrt{Z}) + \xi_b (d_c/d_m)^2 \psi \sqrt{(2rgH)}/(w_1 \sin b_2 \sqrt{Z_c})].$$

The criterion in eq. [41] is simple to use and includes all rational dependencies of the whirl on the system design parameters. It is applicable, however, for very flexible rotors. The relation of the LSC to the Thomas criterion Th and the Torque Deflection Number TDN is,

$$\text{LSC} = \text{Th}[K(\omega/\omega_n)\theta]/[k(\omega C/k - \omega_n/\omega)] = \text{TDN}[\mu K(\omega/\omega_n)\theta]/[2\pi hk(\omega C/k - \omega_n/\omega)] \quad (42)$$

In large steam turbines $\omega Ck \gg \omega_n/\omega$ (eqs. [40], [41]) can be simplified further:

$$\text{LSC} = T\mu K/(hd_m k\omega_n C) = Th(K\theta)/(C\omega_n) = \text{TDN}(\mu K\theta)/(2\pi h\omega C) \quad (43)$$

To observe the system stability behavior, eq. 39 is set at the threshold in the form

$$\eta p_r - p_r^3 = (\alpha + 1)\beta_L \quad (44)$$

The quantity on the right hand side is the limiting excitation parameter, adjusted to the bearing whirl by way of the multiplier $(\alpha + 1)$. The quantity on the left depends on the bearing damping parameter η and the relative whirl frequency p_r, Figure 9. One can observe that the damping required for a given value of the adjusted excitation parameter $(\alpha + 1)\beta_L$ has a minimum value in the range $p_r = 2$ to 4. This is the range of the natural frequency ratios for most machines. For any value of the adjusted excitation parameter, corresponding to a certain machine load, there is a minimum in that range. This can be found by differentiation of eq. [41] is respect to p_r. This yields the optimum value

$$p_r^2 = \eta/3 \quad (45)$$

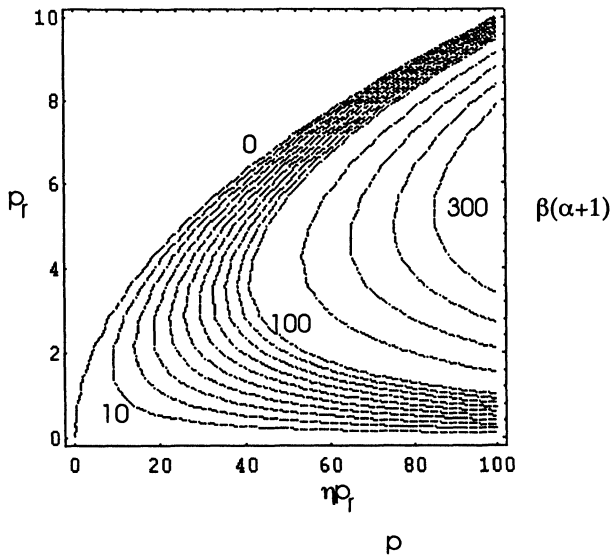

FIGURE 9 Load stability criterion chart. Linear threshold of instability β_L.

CONCLUSION

In this work, a qualitative study was undertaken for the whirl which appears in certain turbomachinery at high loads. The problem has been reduced to a small number of parameters for an ideal system configuration. Stability charts have been plotted for areas of practical interest and the effect of the main governing parameters, namely steam force gradients, internal damping, rotor flexibility and bearings, have been studied. It was shown that the most important parameters are the bearings, from the point of view of both effect on stability and possibility of stabilizing an unstable machine. It was shown that previously used criteria, such as the Torque Deflection Criterion and the Thomas Criterion are either misleading or inadequate for prediction of stability behavior.

It was shown that the damping of the bearing alone does not characterize its capability of absorbing energy. Instead, a damping function was proposed, which takes into account the bearing stiffness, to which stability is inversely proportional. Further, the onset of instability due to steam whirl, one should not expect large amplitudes, as predicted by the linear analysis. In fact, limit orbits are developing which grow with further increase of the load at an accelerated rate. The real range of operation of the machine, stable in engineering terms, is thus extended considerably beyond the linear analysis. One should expect, however, that for the purpose of tabulating the operating experience in similar machines, the Load Stability Criterion proposed here, based on linear analysis, is adequate.

Nomenclature

B_p	dynamic pad load coefficient
C	bearing damping
C_m	is the machined radial clearance of pad
C_2	absolute exit velocity
D	$2R$ is the journal diameter
E_p	$1 - H_p/C_m$, the eccentricity ratio at the pivot point
F_i	force in the direction of coordinate i

H	adiabatic drop of stage
H_p	the oil-film thickness at the pivot point
K	bearing stiffness
K_2	second bearing coefficient
K_3	third bearing coefficient
L	the journal length
N	power
S	bearing force derivatives
T	stage torque
U	peripheral force of the stage
X_i	rotor displacement along coordinate i
W_p	static pad load at the pivot point
Z	number of seal teeth
Z_c	the number of teeth over the blade cover
$a, b, c, m, n, a_k,$ b_k, c_k, m_k, n_k	pad bearing parameters
a_2	exit angle
b_2	stage entrance angle
d_c	outer diameter of the stage = $h + d_m$
d_m	pitch diameter of stage
d_n	shaft diameter
e	rotor eccentricity
g	acceleration of gravity
h	nozzle height
k	rotor stiffness
k_{st}	Thomas follower-force gradient due to flow
m	rotor mass
n	rotating speed, Hz
p	complex whirl frequency ratio ($\omega_W/\omega = (\omega_r + i\omega_i)/\omega$
p_i	imaginary component of whirl frequency ratio ω_i/ω
p_r	real component of whirl frequency ratio ω_r/ω
q	efficiency sensitivity = $\Delta E_{\text{loss}}/\Delta c$
r	the reaction of the stage
$y_{\max}$	static deflection of rotor due to its own weight
w_1	stage entrance velocity
z	complex rotor displacement
Δc	change in stage clearance
ΔE_{loss}	change is stage loss due to Δc
α	K/k, bearing over shaft stiffness ratio
β	k_{st}/k, follower-flow force gradient ratio
β_L	linear threshold of the follower-flow force gradient ratio
γ	$(K_3/k)C_m^2$, 3rd-order bearing nonlinearity ratio
δ	complex journal displacement
ζ	z/C_m, dimensionless rotor amplitude
η	$\alpha\omega C/K$, damping parameter
θ	logarithmic decrement of rotor natural vibration
λ	ω/ω_n, operating frequency ratio
ξ	oil viscosity
ξ_s and ξ_b	calibration constants determined experimentally
τ	ωt, dimensionless time
ϕ	stage velocity coefficient
ω	shaft angular velocity
ω_k	shaft critical speed velocity
ω_n	shaft natural frequency at running speed

References

Alford, J. S., 1965. Protecting Turbomachinery from Self-excited Rotor Whirl, *ASME Transactions, Journal of Engineering for Power,* October, p. 333.

Andritsos, F. E., and Dimarogonas, A. D., 1980. Nonlinear Pad Functions for Static Analysis of Tilting Pad Bearings, ASME Transactions, *Journal of Lubrication Technology,* January, pp. 25–33.

Awrejcewicz J., and Mrozowski, J., 1989. Bifurcations and Chaos of a Particular Van der Pol-Duffing Oscillator, *Journal of Sound and Vibration,* Vol. **132,** No. 1, pp. 89–100.

Baumgartner, M., 1987. Evaluation of Existing Forces in Turbomachinery Induced by Flow in Labyrinth Seals, *ASME Biennial Conference on Mechanical Vibration and Noise,* pp. 337–344. Boston, September.

Benckert, H., 1980. Stromungsbedingte federkennwerte in labyrinthdichtungen, *Doctoral dissertation,* University of Stuttgart.

Black, H. F., 1969. Effects of Hydraulic Forces in Annular Pressure Seals on the Vibrations of Centrifugal Pump Rotors, *Proceedings, IME, Journal of Mechanical Engineering Science,* Vol. **11,** No. 2, p. 206.

Black, H. F., 1970. Dynamic Hybrid Bearing Characteristics of Annular Controlled Leakage Seals, *Proceedings, IME, Journal of Mechanical Engineering Science,* Vol. **184,** pt 3 N, pp. 92–100.

Black, H. F., 1974. Lateral Stability and Vibrations of High Speed Centrifugal Pump Rotors, *IUTAM Symposium on Dynamics of Rotors,* Springer Verlag, Berlin.

Childs, D. W., 1977. The Space Shuttle Main Engine-High Pressure Fuel Turbopump Rotor Dynamic Instability Problem, *ASME Paper No. 77-GT-49,* pp. 27–31. *Gas Turbine Conference, Philadelphia,* March.

Childs, D. W., 1983. Finite-length Solutions for Rotor Dynamic Coefficients of Turbulent Annular Seals, *ASME Transactions, Journal of Lubrication Technology,* Vol. **105,** July 1983, p. 437.

Childs, D. W., 1989. Fluid-Structure Interaction Forces at Pump-Impeller-Shroud Surfaces for Rotor Dynamic Calculations, *ASME Transactions, Journal of Vibrations, Acoustics, Stress and Reliability in Design,* Vol. **111,** July 1989, p. 216.

Childs, D. W., 1993 *Turbomachinery Rotordynamics.* New York: John Wiley.

Childs, D. W., and Kim, C. H., 1985. Analysis and Testing for Rotor Dynamic Coefficients of Turbulent Annular Seals with Different, Directionally-homogeneous Surface Roughness Treatment for Rotor and Stator Elements, *ASME Transactions, Journal of Tribology,* July 1985, Vol. **107.** pp. 296–306.

Childs, D. W., and Scharrer, J. K., 1988. Theory versus Experiment for the Rotor Dynamic Coefficient of Labyrinth Gas Seals: Part II—A Comparison to Experiment, *ASME Transactions, Journal of Vibration, Acoustics, Stress, and Reliability in Design,* Vol. **110,** p. 281.

Childs, D. W., and Scharrer, J. K., 1986(a). An Iwatsubo-based Solution for Labyrinth Seals: Comparison to Experimental Results, *ASME Journal of Engineering for Gas Turbines and Power,* Vol. **108,** No.2, pp. 325–331.

Childs, D. W., and Scharrer, J. K., 1986b. Experimental Rotor Dynamic Coefficient Results for Teeth-on-Rotor and Teeth-on-Stator Labyrinth Gas Seals, *ASME Journal of Engineering for Gas Turbines and Power,* Vol. **108,** No.2, p. 599. Clayton Labs. 1989. *RODYNA*—Users Manual St. Louis, Missouri.

Clayton Labs., 1989. *RODYNA*—Users Manual. St. Louis, Missouri.

Dietzen, F. J., and Nordmann, R., 1987. Calculating Rotor Dynamic Coefficients of Seals by Finite Difference Techniques, *ASME Transactions, Journal of Tribology,* Vol. **109,** p. 388.

Diewald, W., and Nordmann, R., 1987. Dynamic Analysis of Centrifugal Pump Rotors with Fluid Mechanical Interactions, *ASME Biennial Conference on Mechanical Vibration and Noise,* pp. 571–580. Boston, September.

Dimarogonas, A. D., 1971a. Analysis of Steam Whirl, *General Electric Technical Information Series, DF-71-LS-48,* Schenectady, NY.

Dimarogonas, A. D., 1971b. Analysis of Steam Whirl II: Adiabatic Steam Flow between Eccentric Rotating Cylinders, *General Electric Technical Information Series, DF-71-LS-115,* Schenectady, NY.

Dimarogonas, A. D., 1972. A Linear Rotor Stability Analysis, *General Electric Technical Information Series, DF-72-LS-32,* Schenectady, NY.

Dimarogonas, A. D., 1975. A General Method for Stability Analysis of Rotating Shafts, *Ingenieur Archiv,* Vol. **44,** pp. 9–20.

Dimarogonas, A. D., 1976. *Vibration Engineering.* Minneapolis: West Publishing Co.

Dimarogonas, A. D., 1987. Limit Cycles for Pad Bearings under Fluid Excitation, *STLE Transactions.* Vol. **31,** No. 1, pp. 66–70.

Dimarogonas, A. D., 1989. *Computer Aided Machine Design.* Prentice-Hall International London.

Dimarogonas, A. D., 1993. MELAB: *Computer Programs for Mechanical Engineers,* Englewood Cliffs N.J. Prentice-Hall.

Dimarogonas, A. D., and Andritsos, F. E., 1986. Nonlinear Pad Functions for Dynamic Analysis of Tilting Pad Bearings, *ASME Transactions, Journal of Lubrication Technology,* November.

Dimarogonas, A. D. and Haddad, S. D., 1992. *Vibration for Engineers.* Prentice-Hall, Englewood Cliffs. NJ.

Dimarogonas, A. D., and Paipetis, S. A., 1983. *Analytical Methods in Rotor Dynamics,* Applied Science Publishers, London.

Ehrich, F. F., 1972. Identification and Avoidance of Instabilities and Self-excited Vibrations in Rotating Machinery, *ASME Paper No. 72-DE-21,* Design Engineering Conference and Show, Chicago, May.

Ehrich, F. F., 1988. A State-of-the-Art Survey in Rotor Dynamics–Nonlinear and Self-excited Vibration Phenomena. *International Symposium on Transport phenomena, Dynamics and Design of Rotating Machinery,* Dynamics of rotating machinery, p. 3, Honolulu, HI.

Ehrich, F. F., and Childs, D. W., 1984. Self-excited Vibration in High-Performance Turbomachinery, *Mechanical Engineering,* May 1984, p. 66.

Elrod, D. A., Childs, D. W., and Nelson, C. C., 1990. An Annular Gas Seal Analysis Using Empirical Entrance and Exit Region Friction Factors, ASME Transactions, *Journal of Tribology,* Vol. **112,** p. 197.

Elrod, D. A., Childs, D. W., and Nelson, C. C., 1989. An Entrance Region Friction Factor Model Applied to Annular Seal Analysis: Theory versus Experiment for Smooth and Honeycomb Seals, *ASME Transactions, Journal of Tribology,* Vol. **112,** p. 197.

Flack, R. D., and Zuck, C. J., 1987. Experiments on the Stability of Two Flexible Rotors in Tilting-pad bearings, *ASLE Transactions,* 87-AM-3a-1.

Föppl, A., 1895. Das problem Der Lavalschen turbinenwelle, *Der Civilingenier,* Vol. **41,** p. 333.

Fowlie, D. W., and Miles, D. D., 1975. Vibration Problems with High Pressure Centrifugal Compressors, *ASME Paper 75-Pet-28, Petroleum Mechanical Engineers Conference,* Tulsa, OK, September.

Gash, R., 1965. Stabiler Lauf von Turbinenrotoren, *Konstruction,* Vol. **17,** p. 11.

Holmes, R., and Sykes, E. H., 1989. Large Amplitude Vibration in Rotor Assemblies, *Journal of Sound and Vibration,* Vol. **133,** No. 2, pp. 337–351.

Iwatsubo, T., and Yang, B. S., 1988. The Effects of Elastic Deformation on Seal Dynamics, *ASME Transactions, Journal of Vibrations, Acoustics, Stress and Reliability in Design,* Vol. **110,** p. 59.

Kim, C. H., and Childs, D. W., Analysis for Rotor Dynamic Coefficients of Helically-Grooved Turbulent Annular Seals, ASME Transactions, *Journal of Tribology,* Vol. **109,** January 1987, p. 137.

Kirk, R. G., 1988. Aerodynamic Instability mechanisms for Centrifugal Compressors, *Second International Symposium on Rotating Machinery,* pp. 315–326, Honolulu.

Kirk, R. G., and Miller, W. H., 1979. The Influence of High Pressure Oil Seals on Turborotor Stability, *ASLE Transactions,* Vol. **22,** No. 1, pp. 14–24.

Kirk, R. G., and Reddy, S. W., 1988. Evaluation of Pivot Stiffness for Typical Tilting-Pad Journal Bearing Designs, *ASME Transactions, Journal of Vibrations, Acoustics, Stress and Reliability in Design,* Vol. **110,** p. 105.

Kraemer, E., 1968. Selbsterregte Schwingungen, *Brennstoffe-Waerme-Kraft,* Vol. **20,** p. 7.

Landzberg, A. H., 1960. Stability of a Turbine-Generator Rotor Including the Effects of Certain Types of Steam and Bearing Excitation, *ASME Transactions, Journal of Applied Mechanics,* September, p. 410.

Lund, J., 1965. *Design Handbook for Fluid Film Bearings,* AFAPL-TR-65-45. Latham, N.Y.: Mechanical Technology Inc.

Nelson, C. C., 1984. Analysis for Leakage and Rotor Dynamic Coefficients of Surface Roughened Tapered Annular Gas Seals, *ASME Transactions, Journal of Engineering for Power,* Vol. **106,** No. 4. pp. 927–934.

Nelson, C. C., 1985. Rotor Dynamic Coefficients for Compressible Flow in Tapered Annular Seals, *ASME Transactions,* Vol. **107,** pp. 318–325.

Nelson, C. C., and Nguyen, D. T., 1987. Comparison of Hirs' Equation with Moody's Equation for Determining Rotor Dynamic Coefficients of Annular Pressure Seals, *Journal of Tribology,* Vol. **109,** p. 145.

Nicholas, J. C., Gunter, E. J., Allaire, R. E., 1979. Stiffness and damping coefficients for the 5-pad Tilting Pad Bearing. *ASLE Transactions,* Vol. **22,** No. 2, April, pp. 113–124.

Nordman, R., Dietzen, F. J., and Weiser, H. P., 1987. Calculation of Rotor Dynamic Coefficients for Annular Gas Seals by Means of Finite Difference Techniques, *ASME Biennial Conference on Mechanical Vibration and Noise,* pp. 351–358, Boston.

Nordmann, R., and Dietzen, F. J., 1988. Finite Difference Analysis of Rotor Dynamic Seal Coefficients for an Eccentric Shaft Position. International Symposium on Transport Phenomena, Dynamics and Design of Rotating Machinery, *ISROMAC—Dynamics of Rotating Machinery Conference,* p. 193, Honolulu, HI.

Orcutt, F. K., 1989. The steady state and dynamic characteristics of the Tilting Pad Journal Bearings in Laminar and Turbulent Flow Regimes. *ASME Journal of Lubrication Technology,* Vol. **89,** No. 3, pp. 392–404.

Pfleiderer, C., 1952, *Stroemungsmachinen,* Berlin: Springer.

Pollman, E., Schwerdtfeger, H., and Termuehlen, H., 1977. Flow Excited Vibrations in High Pressure Turbines (Steam Whirl), *ASME Transactions, Journal of Engineering for Power,* April, pp. 219–228.

Rajakumar, C., and Sisto, F., 1990. Experimental Investigations of Rotor Whirl Excitation Forces Induced by Labyrinth Seal Flow, *ASME Transactions, Journal of Vibration and Acoustics,* Vol. **112,** pp. 515–522.

Ruhl, R. L. and Booker, J. F., 1971. A Finite Element Model for Distributed Parameter Turborotor Systems, *ASME paper 71-Viber-56.*

Scharrer, J. K., 1988. Theory versus Experiment for the Rotor Dynamic Coefficients of Labyrinth Gas Seals: Part I—A Two Control Volume Model, *ASME Transactions, Journal of Vibrations, Acoustics, Stress and Reliability in Design,* Vol. **110,** p. 270.

Scharrer, J. K., and Nelson, C. C., 1991. Rotor Dynamic Coefficients for Partially Tapered Annular Seals: Part I—Incompressible Flow, *Transactions ASME, Journal of Tribology,* Vol. **113,** p. 48.

Scharrer, J. K. and Nelson, C. C., 1991. Rotor Dynamic Coefficients for Partially Tapered Annular Seals: Part II—Compressible Flow, Transactions ASME, *Journal of Tribology,* Vol. **113,** p. 53.

Shapiro, W., and Colsher, R., 1977. Rotor Whirl in Turbomachinery, Mechanisms, Analyses and Solution Approaches, *ASME Winter Annual Meeting,* Atlanta, November.

Tam, L. T., Przekwas, A. J. Muszynska, A., Braun, M. J., and Mullen, R. L., 1988. Numercial and Analytical Study of Fluid Dynamic Forces in Seals and Bearings, *ASME Transactions, Journal of Vibration, Acoustics, Stress, and Reliability in Design,* Vol. **110,** pp. 315–325.

Thomas, H. J., 1956. Unstable Oscillations of Turbine Rotors Due to Steam Leakage in the Clearances of Rotor and Bucket Packings, *AEG Technical Publication No. 1150.*

Thomas, H.-J., 1958. Unstable Oscillations of Turbine Rotors Due to Steam Leakage in the Clearance of the Sealing Glands and the Buckets, *Bulletin Scientifique, A. J. M.,* Vol. **71,** pp. 1039–1063.

Thompson, J. M. T., and Steward, H. B., 1986. *Nonlinear Dynamics and Chaos.* New York: Wiley Interscience.

Vance, J. M., 1988. *Rotor Dynamics of Turbomachinery.* New York: John Wiley.

Vance, J. M., and Laudadio, F. J., 1984. Experimental Measurement of Alford's Force in Axial Flow Turbomachinery, *ÀSME Transactions, Journal of Engineering for Gas Turbines and Power,* July, pp. 585–590.

Vogel, D. H., 1970. *The Stability of Turbomachine Rotors on Journal Bearings,* Dissertation, Technical University of Munich.

Vogel, D. H., 1970. The Vibration and Stability Behavior of Unbalanced Multi Span Shafts, *Konstruction,* Vol. **22,** p. 12.

Wang, J. H., and Tsai, M. T., 1989. Instability Due to Fluid Leakage of a Rotor system with Anisotropic Support, *ASME Transactions, Journal of Vibrations, Acoustics, Stress and Reliability in Design,* Vol. **111,** January, p. 27.

Wang F. S., Chang, C. S., and Gong, H. S., 1988. An Analysis of the Stability of Rotor System Supported by the Tilting Pad Bearing under Aerodynamic Excitation, *International Symposium on Transport Phenomena, Dynamics and Design of Rotating Machinery, Dynamics of Rotating Machinery,* p. 287, Honolulu, HI.

Warner, R. E., and Soler, A. I., 1975. Stability of Rotor-Bearing Systems with Generalized Support Flexibility and Damping and Aerodynamic Cross-Coupling, *ASME Transactions Journal of Lubrication Technology,* July, p. 461.

Weiser, P., and Nordmann, R., 1989. Calculation of Rotor Dynamic Coefficients for Labyrinth Seals using a 3-D Finite Difference Method, 1989, *ASME Biennial Conference on Mechanical Vibration and Noise,* pp. 109–114, Montreal, Quebec. September.

Wright, D. V., 1977. Air Model Tests of Labyrinth Seal Forces on a Whirling Rotor, *ASME Winter Annual Meeting,* Atlanta, November.

Wright, T., 1984. Axial Fan Performance with Blade-Base Clearance, *ASME Transactions, Journal of Engineering for Gas Turbines and Power,* Vol. **106,** October, p. 901.

Wyssmann, H. R., 1987. Rotor Stability of High Pressure Multistage Centrifugal Compressors, *ASME Biennial Conference on Mechanical Vibration and Noise,* pp. 561–569, Boston, September.

Wyssmann, H. R., and Jenny, R. J., 1984. Prediction of Stiffness and Damping Coefficients for Centrifugal Compressor Labyrinth Seals, *ASME Transactions, Journal of Engineering for Gas Turbines and Power,* October, pp. 920–926.